Soil heat extremes outpace their atmospheric counterpart

Almudena Garcia-Garcia (almudena.garcia-garcia@ufz.de)
Department of Remote Sensing, Helmholtz Centre for Environmental Research - UFZ and Remote Sensing Centre for Earth System Research, Leipzig University

Francisco José Cuesta-Valero
Department of Remote Sensing, Helmholtz Centre for Environmental Research - UFZ and Remote Sensing Centre for Earth System Research, Leipzig University

Diego Miralles
Ghent University https://orcid.org/0000-0001-6186-5751

Miguel Mahecha
Universität Leipzig https://orcid.org/0000-0003-3031-613X

Johannes Quaas
Universitaet Leipzig https://orcid.org/0000-0001-7057-194X

Markus Reichstein
Max Planck Institute for Biogeochemistry, Jena https://orcid.org/0000-0001-5736-1112

Jakob Zscheischler
Helmholtz Centre for Environmental Research https://orcid.org/0000-0001-6045-1629

Jian Peng
Department of Remote Sensing, Helmholtz Centre for Environmental Research - UFZ and Remote Sensing Centre for Earth System Research, Leipzig University

Article

Keywords: Hot extremes, soil moisture-temperature feedback, land-atmosphere interactions, climate change, CMIP6-SSP5

Posted Date: May 16th, 2023

DOI: https://doi.org/10.21203/rs.3.rs-2832579/v1

Additional Declarations: There is **NO** Competing Interest.

Soil heat extremes outpace their atmospheric counterpart

Almudena García-García[1,2*], Francisco José Cuesta-Valero[1,2], Diego G. Miralles[3], Miguel D. Mahecha[1,2], Johannes Quaas[4], Markus Reichstein[5], Jakob Zscheischler[6] and Jian Peng[1,2*]

[1*]Department of Remote Sensing, Helmholtz Centre for Environmental Research - UFZ, Leipzig, Germany.
[2]Remote Sensing Centre for Earth System Research, Leipzig University, Leipzig, Germany.
[3]Hydro-Climate Extremes Lab (H-CEL), Ghent University, Ghent, Belgium.
[4]Leipzig Institute for Meteorology, Leipzig University, Leipzig, Germany.
[5]Department of Biogeochemical Integration, Max Planck Institute for Biogeochemistry, Jena, Germany.
[6]Department of Computational Hydrosystems, Helmholtz Centre for Environmental Research , Leipzig, Germany.

*Corresponding author(s). E-mail(s):
almudena.garcia-garcia@ufz.de; jian.peng@ufz.de;
Contributing authors: fjcuestavalero@ufz.de;
Diego.Miralles@UGent.be; miguel.mahecha@uni-leipzig.de;
johannes.quaas@uni-leipzig.de; mreichstein@bgc-jena.mpg.de;
jakob.zscheischler@ufz.de;

Abstract

Hot temperature extremes are changing in intensity and frequency. Quantifying these changes is key for developing adaptation strategies [1]. The conventional approach to study changes in hot extremes is based on air temperatures. However, hydrology [2] and many biogeochemical processes, e.g. decomposition of organic material and release

of CO_2 [3]- are more sensitive to soil rather than air temperature. In this study, we show that soil hot extremes are increasing faster than air hot extremes by $\mathbf{0.7°C/Decade}$ in intensity and twice as fast in frequency on average over Central Europe. Furthermore, we identify soil temperature as a factor in the soil moisture–temperature feedback. During dry conditions, increases in net radiation yield higher soil temperature and a consequent release of sensible heat while latent heat flux is constrained by soil moisture deficits. The release of sensible heat from soils leads to increases in air temperature and vapour pressure deficit that may further dry out and warm up the soil. This study further highlights the contribution of soil moisture–temperature feedback to the evolution of hot extremes in a warming climate. The rapid increase in soil heat extremes shown in these results may have important implications for climate and ecological risk applications.

Keywords: Hot extremes, soil moisture–temperature feedback, land–atmosphere interactions, climate change, CMIP6-SSP5

1 Introduction

Extreme temperatures and associated disasters, such as crop loss, wildfires, water scarcity, air pollution and CO2-release from ecosystems, exert a heavy toll on society and ecosystems [4–7]. For example, a death toll of 55,000, more than 1 million ha of burned land, and US$15 billion of total economic loss were associated with the 2010 Russian heatwave [5]. A recent study has also related more than 100,000 deaths from 2002 to 2015 to extreme temperatures in Latin American cities [8]. More generally, there is evidence of a positive trend in the intensity and frequency of extreme temperatures at global and regional scales that is increasing public concern [1].

Despite the negative consequences of heatwaves and the observed trends in their occurrence and evolution, our understanding of how climate change may affect them is still limited [9]. This is in part caused by the incomplete knowledge of processes controlling the evolution of heat extremes, such as land–atmosphere coupling. This knowledge gap is illustrated, for example, in

the different levels of land–atmosphere coupling represented in climate models [10, 11]. Land conditions can intensify and propagate heatwaves via diabatic heating [12], in the worst case leading to mega-heatwaves [13]. In the presence of persistent high-pressure systems, soil moisture deficits and their induced reduction in evaporation may lead to the warming of the land and a larger fraction of net radiation dissipated as sensible heat into the atmosphere [14]. This directly contributes to the development or intensification of local heatwaves as measured by surface air temperatures, and may further increase soil desiccation [15] and extreme temperatures [13] in downwind areas. Therefore, the observed and projected changes in soil conditions under climate change have been proposed as an important driver of future changes in the intensity and frequency of heatwaves via shifts in the energy partition at the land surface [14].

Although soil temperature links soil moisture and air temperature and is one of the main drivers of the terrestrial carbon cycle, the study of the more direct role of soil temperature in land–atmosphere feedbacks has not received as much attention as the role of soil moisture dynamics [9, 14]. This is partially due to the tight coupling between air and soil temperatures at climate scales [16]. However, the relationship between air and soil temperatures is largely influenced by changes in land cover, aerodynamic conductance, soil water content and associated changes in soil properties [17]. Higher warming rates in soil than air have been already recorded in China [18] and Germany [19], with meteorological stations in China also reporting different trends in maximum soil and air temperatures [20].

Here, we explore the evolution of soil hot extremes over Europe during the last decades, and compare this evolution with that of hot extremes

based on near surface air temperatures. We provide evidence of regional differences between changes in soil and air hot extremes based on meteorological observations [21–36], remote sensing data [37] and the ERA5Land reanalysis products [38]. Furthermore, simulations from the Earth System Models (ESMs) participating in the sixth phase of the Coupled Model Intercomparison Project (CMIP6) [39] are used to investigate the role of soil temperature in the evolution of near surface extreme temperatures in a warming climate.

2 Soil hot extremes in the recent past

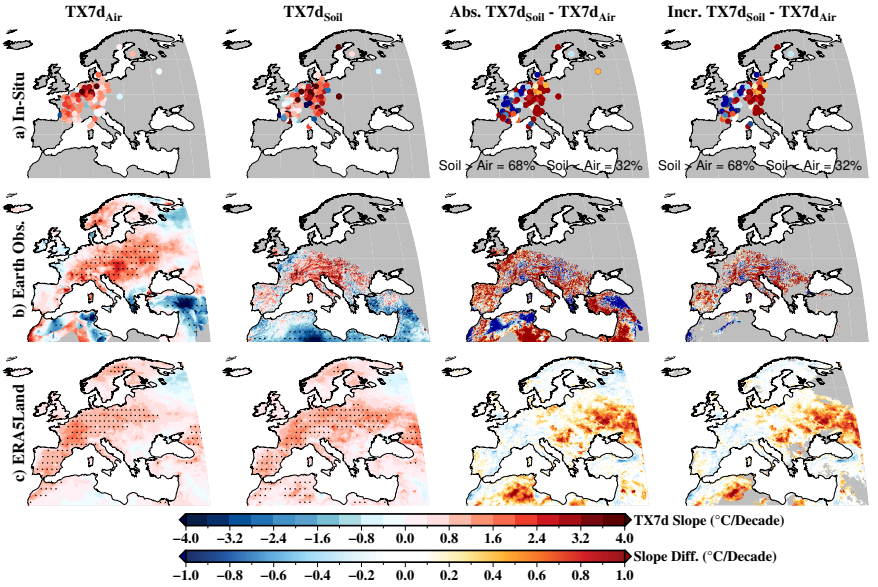

Fig. 1 TX7d trends based on air and soil temperatures from 1996 to 2021 over Europe. From left to right, trend in TX7d based on air temperatures, trend in TX7d based on soil temperatures, the difference between absolute values of trends in soil and air, and the difference between trends in soil and in air where both trends are positive. Results are obtained from meterological stations (a), a combination of CMSAF remote sensing data and the E-OBS gridded dataset (b) and the ERA5Land reanalysis product (c). Gaps in b) correspond with pixels where the gridded product do not match the criteria for estimating trends (see Methods). Dots indicate areas with significant trends above the 90% confidence level.

Trends in the intensity of hot extremes based on air and soil temperatures are investigated using the annual TX7d index defined as the mean of daily maximum temperatures during the hottest week per year. The TX7d trends based on air and soil temperatures based on data from meteorological stations, remote sensing products and reanalysis products show positive trends in air and soil TX7d index from 1996 to 2021 in Central Europe (Figure 1). Trends in soil TX7d show larger spatial variability than in air based on data from meteorological observations (Extended Data Fig. 1), which indicates that local processes and soil heterogeneity have a stronger impact on soil temperature extremes than in air (Fig. 1a). The comparison of TX7d trends in soil and air shows 68% of measurements with larger absolute values of trends in soil than in air, i.e. soil extremes are changing faster than air extremes at those stations. The same percentages are obtained when only observations with positive trends are compared, i.e. 68% of measurements indicate that TX7d trends in soil are increasing faster than for air temperature. Most stations that portray a faster increase in soil than in air temperature extremes are located over Germany, Italy and southern France, while the opposite case is found over central and northern France, Belgium and The Netherlands.

Results from the combination of the E-OBS gridded product [36] and the CMSAF remote sensing data [37] also support the existence of different TX7d trends in air and in the surface. However, remote sensing technologies are not able to derive soil temperatures but surface skin temperatures corresponding with the temperature of each land cover. Positive TX7d trends in skin temperatures are found over Central Europe and along the Mediterranean European coast consistent with the E-OBS map, which suggests that TX7d trends in soil, vegetation and air are mostly driven by climate trends (Fig. 1b). The

comparison of TX7d trends indicates large differences between the land's surface and air, with most areas in Europe showing faster changes in vegetation and/or soil temperatures than in air temperatures. This is also the case when only positive trends are compared. However, some small regions indicate a higher TX7d increase based on air temperatures than on skin temperatures over some forested areas in northeastern Spain, northwestern Italy, southwestern Germany and Greece. Thus, land cover affects the difference between TX7d trends in surface and air, likely indicating a different behaviour over forested areas with skin temperatures corresponding to heights much higher than the land surface. Regions with faster TX7d trends in soil than in air are also found based on the ERA5Land data, which relies on a modelling framework to estimate soil temperature (Fig. 1c). In this dataset, the spatial patterns of TX7d trends in soil and air are very similar, with values much closer than for the observational products. The ERA5land product shows slightly faster increase in air than in soil extreme temperatures over France and the opposite behaviour over eastern Germany and western Poland. Larger differences are found over central-eastern Europe, where TX7d in soil increases faster than in air by more than $0.5°C/Decade$ (Fig. 1c).

Hot extremes are also increasing in frequency using air and soil temperatures over Central Europe (Extended Data Fig. 2). Soil and air differences are consistent and even more robust when using a widely used frequency index for hot extremes; the summer mean of the monthly TX90p index defined as the percentage of days per month when daily maximum temperature is higher than a statistical threshold (Extended Data Fig. 2). In this study, the threshold was estimated as the 90th percentile of daily maximum temperatures for the first 10 years of the period to be able to use the in-situ observations (see Methods for more details). This indicates that the rapid increase in soil heat extremes

in comparison with air heat extremes is independent of the index definition but differences between slopes in soil and air are reliant on the resolution and local characteristics of the data source. Thus, soil hot extremes are increasing $0.7°C/Decade$ faster than air hot extremes in intensity and $5\%/Decade$ faster than air hot extremes in frequency (i.e., twice as fast) on average over Central Europe based on the station data (Extended Data Fig.1).

3 Soil temperature as a factor in the soil moisture–temperature feedback

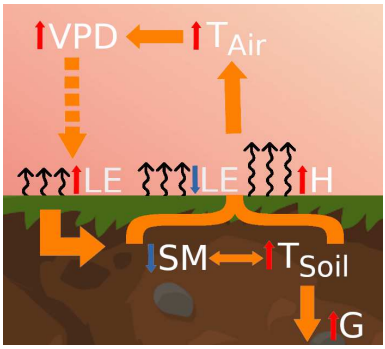

Fig. 2 Soil temperature as a component of the soil moisture–temperature feedback. Due to soil water limitations, an increase in net radiation leads to a rise in soil temperature (T_{Soil}). If soil temperature is higher than the temperature of air above the surface or than deep soil temperatures, the energy absorbed by the soil can be dissipated by conduction in the form of sensible (H) or ground (G) heat, while latent heat flux (LE) is constrained by soil moisture deficits. The release of sensible heat into the atmosphere will increase local and/or remote air temperatures (T_{Air}), leading to vapour pressure deficits (VPD). The increased VPD may in turn increase the demand for latent heat flux, therefore further drying out and warming up the soil. Red (blue) arrows indicate an increase (decrease), while the orange arrows indicates the direction of the feedback.

The evolution of above surface hot extremes is particularly sensible to land–atmosphere interactions over dry or transitional areas during sunny anticyclonic conditions [40]. Under dry soil conditions, the heat capacity of soil can be much lower than under wet conditions [41], favouring the use of net radiation to warm up the soil. If soil temperature is then higher than air temperature

near the land surface, this heat is released from the soil to the atmosphere as sensible heat, since latent heat flux is constrained by soil moisture deficits. If surface soil temperature is warmer than deeper soil temperatures, this temperature can also be propagated through the soil, dissipating heat by conduction and increasing ground heat flux. The fraction of net radiation, that is released in the form of sensible heat into the atmosphere due to the restriction on latent heat flux, will then increase air temperatures. This sensible heat will affect local and/or remote temperatures depending on atmospheric circulation [13]. The increase in air temperatures leads to vapour pressure deficits, which will increase evaporative demand from already dry soils, thus possibly further leading to decreased soil water content and more energy available to warm up soils (Fig. 2). Therefore, soil temperature acts as a factor in the soil moisture–temperature feedback that may reinforce hot spells in the lower atmosphere due to the restrictions on soil moisture and evaporation during extremes. This is the case, for example, at the DE-Tha station located in eastern Germany, where multi-year changes in soil moisture and latent heat flux are restricted during the hottest week of each year, while sensible heat flux and TX7d trends based on air and soil temperatures are significantly increasing during hot extremes in the last decades (Extended Data Fig. 3). The ERA5Land data also support the link between soil temperatures, soil moisture and the evolution of hot extremes above the surface, showing a strong inverse correlation between soil moisture and soil temperature and a strong relationship between air and soil temperatures during TX7d extremes above the surface (Extended Data Fig. 4).

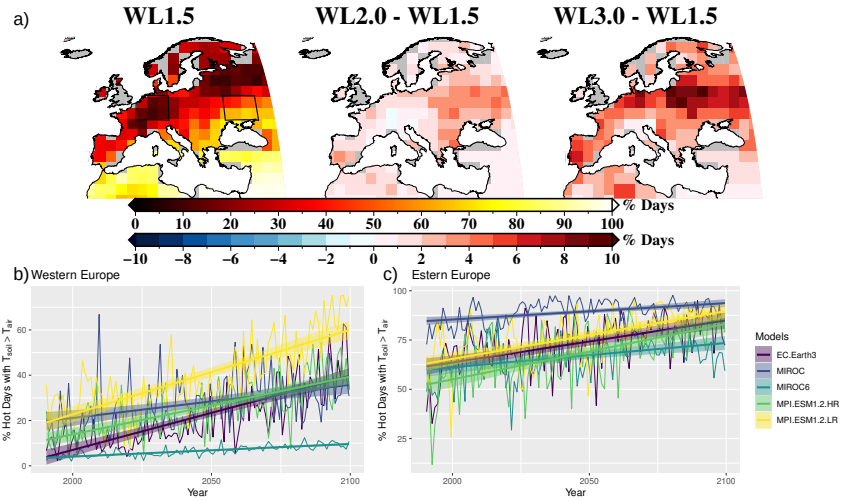

Fig. 3 Percentage of days with a release of heat from soil into the atmosphere in summer. a) Percentage of days with maximum soil temperatures higher than maximum air temperatures during air hot extremes as represented by the multimodel mean of the CMIP6 models under the 1.5 $°C$ warming level and its difference with warming levels of 2.0 $°C$ and 3.0 $°C$. Air hot extremes are defined based on the TX90p index in June, July and August. Averaged percentage of days per year with soil temperatures higher than air temperatures during air hot extremes over central-eastern (b) and western (c) Europe (see black rectangles at top left) from 1990 to 2100 for each model separately.

4 The role of soil temperatures in a warming climate

When the soil surface is warmer than the air above the surface, there is a heat exchange from the soil to the lower atmosphere in the form of sensible heat. This release of heat can contribute to the intensification and spreading of air hot extremes and heatwaves [42]. To investigate the possible contribution of soil temperatures to hot extremes near the surface in the future, the percentage of days with daily maximum soil temperatures higher than daily maximum air temperatures during air hot extremes were estimated. That is, the percentage of days when soil is releasing energy into the atmosphere during air hot extremes, not just during night but also at peak temperatures. The historical and SSP5-8.5 experiments from five CMIP6 models were used to study the change in the probability of occurrence of these events. Although there are

large differences between climate models in simulating future conditions, particularly when soil processes are involved [11], we study the probability of these events, being consistent with the physics of each individual model. Then, we investigate the agreement among models in the effect of climate change on the probability of events when soil temperatures are reinforcing air hot extremes.

The CMIP6 models show a higher number of days with warmer soils than air during hot spells over Mediterranean areas and central-eastern Europe with an increasing trend over the whole Europe, during the 21st century (Fig. 3a). The changes in the percentage of days when soil temperature reinforces near surface hot spells under the 2.0 $^{\circ}C$ and 3.0 $^{\circ}C$ warming levels in comparison with the 1.5 $^{\circ}C$ warming level, show larger changes in Central Europe, and particularly larger over eastern Europe, reaching regional differences between the 3.0 and 1.5 warming levels of more than 8% of hot days (Fig. 3). The spatial averages of the percentage of days when soil temperature reinforces hot spells over central-eastern and western Europe show some disagreement between models in the total number of days when these events happen. There is, however, unanimity among models in the increase in the probability of the occurrence of these events, although with different rates between models (Fig. 3). For example, in eastern Europe, all models indicate more than 10% increase in the days with a contribution of soil temperatures to hot spells at the end of the 21st century than in 1990 under the SSP5-8.5 emission scenario (Fig. 3b). In western Europe, four out of five models also indicate an increase of more than 10% in the days when soil temperature reinforces hot spells at the end of the 21st century (Fig. 3c). Similar conclusions are reached when comparing daily mean air and soil temperatures during hot spells based on maximum air temperatures, showing more consistency among models and larger trends, particularly in eastern Europe (Extended Data Fig. 5), which indicates the robustness of these results.

5 Implications

Our results reveal that soil hot extremes are intensifying and becoming more frequent than air hot extremes at local and regional scales over Europe, particularly over Central Europe. These regional differences between air and soil hot extremes are of particular relevance for impact studies on agriculture and terrestrial ecosystem functions. Current impact and risk studies are usually based on surface air temperature observations [e.g. 43] due to the larger data availability above the land surface than within soil. In light of these results, studies on the impacts of hot extremes on agricultural activities and the terrestrial carbon budget based on air temperatures may underestimate the implications of the rapid increase in soil hot extremes. Thus, maximum soil temperatures should be included in impact and risk studies as a complementary perspective to the traditional approach. Our findings further support the importance of the soil moisture–temperature feedback for the evolution of hot spells in a warming climate. Although all models indicate an increase in days when soil temperatures may reinforce hot spells via the soil moisture–temperature feedback, large differences between models were found. Thus, the representation of soil temperature and its role in the soil moisture –temperature feedback within climate models will have to be examined and improved in order to infer the exact contribution of soil temperatures to future hot extremes and heatwaves.

Supplementary information.

Acknowledgments.

Declarations

- Funding
  Francisco José Cuesta-Valero is an Alexander von Humboldt Research Fellow at the Helmholtz Centre for Environmental Research (UFZ)
- Conflict of interest/Competing interests (check journal-specific guidelines for which heading to use)
- Ethics approval

- Consent to participate
- Consent for publication
- Availability of data and materials
  In situ measurements were obtained from the FLUXNET2015 dataset [21], the Integrated Carbon Observation System network (ICOS) [22–32], the Agenzia Regionale per la Prevenzione e Protezione Ambientale del Veneto (ARPAV, [33]), Deutscher Wetterdienst [34] and from Météo France [35]. The CM SAF Land Surface Temperature dataset is available from https://www.cmsaf.eu/. The E-OBS and ERA5Land variables can be downloaded from the Copernicus Climate Service (https://climate.copernicus.eu/climate-reanalysis). The climate model outputs can be downloaded from the WCRP Coupled Model Intercomparison Project (Phase 6) https://esgf-data.dkrz.de/search/cmip6-dkrz/.
- Code availability
  The TX90 index and thresholds were produced using climdex.pcic in R and available in https://CRAN.R-project.org/package=climdex.pcic.
- Authors' contributions
  AGG downloaded the data, performed the data analysis, produced the figures and wrote the original draft. All authors contributed to develop the final storyline of the paper, and to the final writing and editing of the paper.

References

[1] Seneviratne, S. *et al.* Weather and climate extreme events in a changing climate. In Masson-Delmotte, V. *et al.* (eds.) *Climate Change 2021: The Physical Science Basis. Contribution of Working Group I to the Sixth Assessment Report of the Intergovernmental Panel on Climate Change* (Cambridge University Press, 2021. In Press).

[2] Goebel, M.-O., Bachmann, J., Reichstein, M., Janssens, I. A. & Guggenberger, G. Soil water repellency and its implications for organic matter decomposition – is there a link to extreme climatic events? *Global Change Biology* **17**, 2640–2656 (2011). URL https://onlinelibrary.wiley.com/doi/abs/10.1111/j.1365-2486.2011.02414.x. https://onlinelibrary.wiley.com/doi/pdf/10.1111/j.1365-2486.2011.02414.x.

[3] Fang, C., Smith, P., Moncrieff, J. B. & Smith, J. U. Similar response of labile and resistant soil organic matter pools to changes in temperature. *Nature* **433**, 57–59 (2005). URL https://doi.org/10.1038/nature03138.

[4] Robine, J.-M. *et al.* Death toll exceeded 70,000 in Europe during the summer of 2003. *Comptes Rendus Biologies* **331**, 171–178 (2008).

[5] Barriopedro, D., Fischer, E. M., Luterbacher, J., Trigo, R. M. & García-Herrera, R. The hot summer of 2010: Redrawing the temperature record map of Europe. *Science* **332**, 220–224 (2011). URL https://www.science.

org/doi/abs/10.1126/science.1201224.

[6] Lesk, C., Rowhani, P. & Ramankutty, N. Influence of extreme weather disasters on global crop production. *Nature* **529**, 84–87 (2016).

[7] Salomón, R. L. *et al.* The 2018 European heatwave led to stem dehydration but not to consistent growth reductions in forests. *Nature Communications* **13** (2022).

[8] Kephart, J. L. *et al.* City-level impact of extreme temperatures and mortality in Latin America. *Nature Medicine* (2022).

[9] Miralles, D. G., Gentine, P., Seneviratne, S. I. & Teuling, A. J. Land–atmospheric feedbacks during droughts and heatwaves: state of the science and current challenges. *Annals of the New York Academy of Sciences* **1436**, 19–35 (2019).

[10] Sippel, S. *et al.* Refining multi-model projections of temperature extremes by evaluation against land–atmosphere coupling diagnostics. *Earth System Dynamics* **8**, 387–403 (2017).

[11] García-García, A., Cuesta-Valero, F. J., Beltrami, H. & Smerdon, J. E. Characterization of air and ground temperature relationships within the cmip5 historical and future climate simulations. *Journal of Geophysical Research: Atmospheres* **124**, 3903–3929 (2019).

[12] Röthlisberger, M. & Papritz, L. Quantifying the physical processes leading to atmospheric hot extremes at a global scale. *Nature Geoscience* (2023).

[13] Schumacher, D. L., Keune, J., van Heerwaarden, C. C., Vilà-Guerau de Arellano, J. & Teuling, D. G., Adriaan J.and Miralles. Amplification of mega-heatwaves through heat torrents fuelled by upwind drought. *Nature Geoscience* **12**, 712–717 (2019).

[14] Seneviratne, S. I. *et al.* Investigating soil moisture–climate interactions in a changing climate: A review. *Earth-Science Reviews* **99**, 125–161 (2010).

[15] Schumacher, D. L., Keune, J., Dirmeyer, P. & Miralles, D. G. Drought self-propagation in drylands due to land–atmosphere feedbacks. *Nature Geoscience* **15**, 262–268 (2022).

[16] Smerdon, J. E. *et al.* Daily, seasonal, and annual relationships between air and subsurface temperatures. *Journal of Geophysical Research: Atmospheres* **111** (2006).

[17] Melo-Aguilar, C. *et al.* Near-surface soil thermal regime and land–air temperature coupling: A case study over spain. *International Journal*

of Climatology 1–19 (2022). URL https://rmets.onlinelibrary.wiley.com/doi/abs/10.1002/joc.7662.

[18] Zhang, H., Wang, E., Zhou, D., Luo, Z. & Zhang, Z. Rising soil temperature in China and its potential ecological impact. *Scientific Reports* **6**, 35530 (2016).

[19] Dorau, K., Bamminger, C., Koch, D. & Mansfeldt, T. Evidences of soil warming from long-term trends (1951–2018) in North Rhine-Westphalia, Germany. *Climatic Change* **170** (2022).

[20] Wang, L. *et al.* Maximum and minimum soil surface temperature trends over China, 1965–2014. *Journal of Geophysical Research: Atmospheres* **123**, 2004–2016 (2018).

[21] Pastorello, G. *et al.* The FLUXNET2015 dataset and the ONEFlux processing pipeline for eddy covariance data. *Scientific Data* **7**, 225 (2020). URL https://doi.org/10.1038/s41597-020-0534-3.

[22] Vincke, C. *et al.* Etc l2 meteo, vielsalm, 2019-12-31–2022-09-30 (2022). URL https://hdl.handle.net/11676/fP0w7LtYoUv_qaa90yzCAVVG.

[23] Gharun, M. *et al.* Etc l2 meteo, davos, 2018-12-31–2021-12-31 (2022). URL https://hdl.handle.net/11676/t3hy9SMIg6VP3ilSchHODtJB.

[24] Šigut, L. *et al.* Etc nrt meteosens, bily kriz forest, 2022-05-17–2022-12-11 (2022). URL https://hdl.handle.net/11676/Tn_OAMszm-rS5bBvRm813tFg.

[25] Gianelle, D., Belelli Marchesini, L., Marcolla, B., Sottocornola, M. & ICOS Ecosystem Thematic Centre. Warm winter 2020 ecosystem eddy covariance flux product from monte bondone (2022). URL https://meta.icos-cp.eu/objects/TpS_6HENQSySMMG8jkkAmaJp.

[26] Kruijt, B. & ICOS Ecosystem Thematic Centre. Drought-2018 ecosystem eddy covariance flux product from loobos (2020). URL https://meta.icos-cp.eu/objects/xJKKbVMsJQr-x5vldv08vAUZ.

[27] Nilsson, M. *et al.* Etc nrt meteosens, degero, 2022-08-31–2022-12-11 (2022). URL https://hdl.handle.net/11676/moB5yTHVhT-Sq3aCvmUFmlst.

[28] Montagnani, L. *et al.* Etc nrt meteosens, renon, 2021-11-16–2022-12-11 (2022). URL https://hdl.handle.net/11676/nXoijrJPtQ7pAlqRRF-CRb8u.

[29] Mammarella, I. *et al.* Etc nrt meteosens, hyytiala, 2022-10-31–2022-12-11 (2022). URL https://hdl.handle.net/11676/AsiIMmDR7KdBoo0U3Za8zwyY.

[30] Ibrom, A., Møller, F., Pilegaard, K., Rønn Lange, E. & Schaarup Sørensen, J. Etc nrt meteosens, soroe, 2022-10-31–2022-12-11 (2022). URL https://hdl.handle.net/11676/iR7JTKt9bLSLOKooGUSxEPxh.

[31] Bernhofer, C. *et al.* Etc nrt meteo, tharandt, 2021-12-31–2022-12-11 (2022). URL https://hdl.handle.net/11676/YsYmXilwxqKgGzqSQf7HFhfG.

[32] Brümmer, C. & Delorme, J.-P. Etc nrt meteo, gebesee, 2022-08-31–2022-12-11 (2022). URL https://hdl.handle.net/11676/TKd-wR-smoJFGvis9gsjVogo.

[33] ARPAV, U. O. M., Territorial Security Department & Climatology. Hourly air and soil temperatures from 2000 to 2022 over venice province (2022). URL https://www.arpa.veneto.it/previsioni/it/html/meteo_veneto.php.

[34] DWD. Hourly air and soil temperatures of the climate data center (cdc) of the deutscher wetterdienst (dwd) (2022). URL https://opendata.dwd.de/climate_environment/.

[35] France, M. 6-hr air and soil temperatures from observations in situ (2022). URL https://donneespubliques.meteofrance.fr.

[36] Cornes, R. C., van der Schrier, G., van den Besselaar, E. J. M. & Jones, P. D. An ensemble version of the e-obs temperature and precipitation data sets. *Journal of Geophysical Research: Atmospheres* **123**, 9391–9409 (2018).

[37] Duguay–Tetzlaff, A. *et al.* Cm saf land surface temperature dataset from meteosat first and second generation - edition 1 (sumet ed. 1),. Tech. Rep., Satellite Application Facility on Climate Monitoring (2017).

[38] Muñoz Sabater, J. *et al.* Era5-land: a state-of-the-art global reanalysis dataset for land applications. *Earth System Science Data* **13**, 4349–4383 (2021). URL https://essd.copernicus.org/articles/13/4349/2021/.

[39] Eyring, V. *et al.* Overview of the coupled model intercomparison project phase 6 (cmip6) experimental design and organization. *Geoscientific Model Development* **9**, 1937–1958 (2016). URL https://gmd.copernicus.org/articles/9/1937/2016/.

[40] Quesada, B., Vautard, R., Yiou, P., Hirschi, M. & Seneviratne, S. I. Asymmetric European summer heat predictability from wet and dry southern winters and springs. *Nature Climate Change* **2**, 736–741 (2012).

[41] Abu-Hamdeh, N. H. Thermal properties of soils as affected by density and water content. *Biosystems Engineering* **86**, 97–102 (2003). URL https://www.sciencedirect.com/science/article/pii/S1537511003001120.

[42] Miralles, D. G., Teuling, A. J., van Heerwaarden, C. C. & Vilà-Guerau de Arellano, J. Mega-heatwave temperatures due to combined soil desiccation and atmospheric heat accumulation. *Nature Geoscience* **7**, 345–349 (2014).

[43] Zhao, C. *et al.* Temperature increase reduces global yields of major crops in four independent estimates. *Proceedings of the National Academy of Sciences* **114**, 9326–9331 (2017). URL https://www.pnas.org/doi/abs/10.1073/pnas.1701762114. https://www.pnas.org/doi/pdf/10.1073/pnas.1701762114.

[44] for the Pacific Climate Impacts Consortium, D. B. climdex.pcic: Pcic implementation of climdex routines (2020). URL https://CRAN.R-project.org/package=climdex.pcic.

[45] Tachiiri, K. *et al.* Miroc miroc-es2l model output prepared for cmip6 scenariomip ssp585 (2019). URL https://doi.org/10.22033/ESGF/CMIP6.5770.

[46] Shiogama, H., Abe, M. & Tatebe, H. Miroc miroc6 model output prepared for cmip6 scenariomip ssp585 (2019). URL https://doi.org/10.22033/ESGF/CMIP6.5771.

[47] Wieners, K.-H. *et al.* Mpi-m mpi-esm1.2-lr model output prepared for cmip6 scenariomip ssp585 (2019). URL https://doi.org/10.22033/ESGF/CMIP6.6705.

[48] Schupfner, M. *et al.* Dkrz mpi-esm1.2-hr model output prepared for cmip6 scenariomip ssp585 (2019). URL https://doi.org/10.22033/ESGF/CMIP6.4403.

[49] (EC-Earth), E.-E. C. Ec-earth-consortium ec-earth3 model output prepared for cmip6 scenariomip ssp585 (2019). URL https://doi.org/10.22033/ESGF/CMIP6.4912.

[50] Hauser, M., Engelbrecht, F. & Fischer, E. M. Transient global warming levels for CMIP5 and CMIP6 (2022). URL https://doi.org/10.5281/zenodo.7390473.

Methods

Datasets. Extreme indices are estimated based on maximum air and soil temperatures from different data sources. Sub-daily air and soil temperatures at depths shallower than 15 cm were obtained from the FLUXNET2015 dataset [21], the Integrated Carbon Observation System network (ICOS) [22–32], the Agenzia Regionale per la Prevenzione e Protezione Ambientale del Veneto (ARPAV, [33]), Deutscher Wetterdienst [34] and from Météo France [35]. We obtained instantaneous land surface skin temperatures for the period 1991-2015 from the CM SAF Land Surface Temperature dataset from Meteosat First and Second Generation - Edition 1 [37] and maximum air temperatures from the E-OBS daily gridded land-only observational dataset [36]. From the hourly product of the ERA5Land reanalysis [38], we used air temperatures defined at 2 m of height and soil temperatures and moisture at the first soil layer (0-7 cm).

Extreme Indices. Two definitions of hot extreme indices have been used in this study: 1) TX7d defined as the mean value of daily maximum temperatures over the hottest week per year and relevant as a measure of the intensity of hot extremes. 2) TX90p relevant for the frequency of hot extremes and defined as the percentage of hot days per year. We considered hot days as the days when maximum temperature is above the calendar day 90th percentile centred on a 5-day window for the base period, defined in this study as the first 10 years of the dataset. We estimated daily maximum air and soil temperatures from all databases only at days with the whole representation of the daily cycle according to each data temporal resolution. The TX90 indices were computed using the R package climdex.pcic [44]. The TX7d index was estimated for each year from all databases at stations or pixels with no more than 20 consecutive missing values in the year, while the monthly TX90p index was

estimated only at stations and pixels with less than 30% of data as missing values. The indices were computed for the period 1996-2020 in order to use as many meteorological observations as possible. Thus, the base period used for the TX90p index corresponds to 1996-2005 for the index built on all gridded products, but for each station the base period will change according to the data availability. Then, trends were estimated only at stations and pixels with more than 10 years of data. Trend significance and magnitude in the two extreme indices for all datasets were computed based on the Mann-Kendall trend test and the non-parametric Sen's slope estimator to reduce differences in trends associated with the data availability of each station. Significances were calculated at the 90% confidence level for all datasets and only stations presenting statistically significant trends in at least one of the index based on air or soil temperatures were included in the analysis. Trends in the TX90p index were computed only during boreal summer, calculating the average of the monthly TX90p index in June, July and August (JJA) each year. Thus, TX7d trends were estimated at a total of 132 stations (20 FLUXNET, 11 ICOS, 14 ARPAV, 40 DWD and 47 Météo France) corresponding with 179 pairs of air and soil measurements. Due to the different criteria used for estimating the indices, the number of stations at which TX90p trends were estimated is slightly different, being a total of 103 stations (11 ICOS, 14 ARPAV, 49 DWD and 29 Météo France) corresponding with 154 pairs of air and soil measurements.

Soil moisture–temperature feedback in a warming climate

Outputs of daily maximum air temperature (2 m) and 6-hr soil temperature at 5 cm were obtained from the CMIP6-ESGF archive. Temperature outputs from the historical and SSP5-8.5 simulations were used for each model using the first realization. The number of models included in the analysis based on

soil temperatures is limited to five (MIROC-ES2L [45], MIROC6 [46], MPI-ESM2-LR [47], MPI-ESM2-MR [48] and EC-Earth3 [49]), since only these models provide outputs of sub-daily soil temperatures for the two simulations and they were required to estimate daily maximum soil temperatures. The study of soil temperature as heat contributor to future hot days developed near the surface was performed comparing daily maximum soil and air temperatures during hot days in summer (JJA). Hot days were identified using the monthly TX90p index based on air temperatures. Thus, we estimated the percentage of hot days when maximum soil temperatures are higher than maximum air temperatures, defining hot days with the TX90p index based on air temperatures. The same analysis was done comparing mean daily soil and air temperatures, reaching similar conclusions but higher percentages with mean temperatures than those using maximum temperatures (Extended Data Fig. 5). Results are presented using the multimodel mean, interpolating each final model result to the coarsest grid (MIROC-ES2L). To avoid the effect of the different climate sensitivity of each climate model on the results, we used three different warming levels (1.5, 2.0 and 3.0). Warming levels are estimated for each model realization as suggested by Hauser et al., 2022 [50].

Extended Data Figures

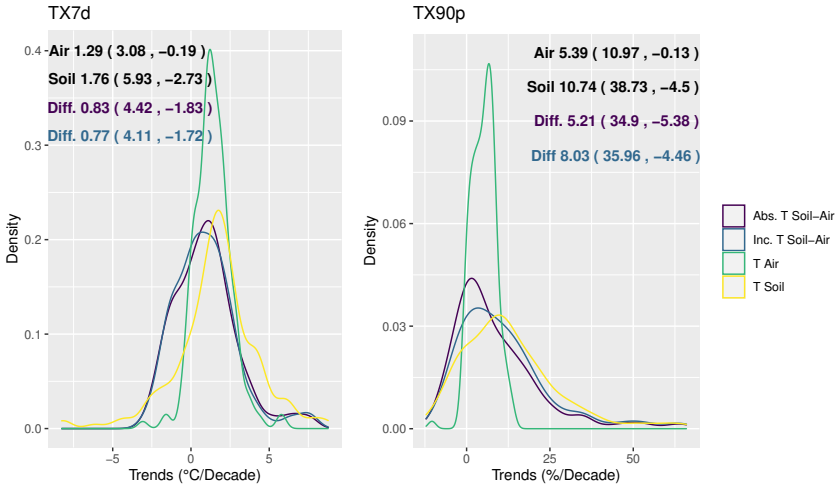

Extended Data Figure 1 | Probability distributions of trends in TX7d and TX90p from in-situ data. Probability distributions of TX7d and TX90p trends based on air and soil observations, the difference of the absolute values of trends in soil and in air and the difference between soil and air trends at stations with positive trends. Numbers indicate the median (95th and 5th percentiles) of the distributions based on air and soil temperatures and the differences between soil and air slopes.

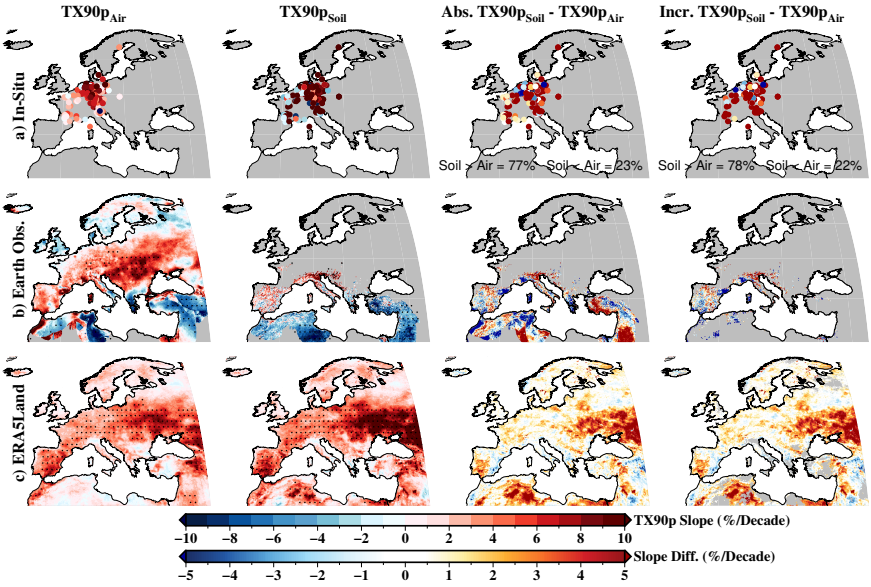

Extended Data Figure 2 | TX90p trends based on air and soil temperatures in summer from 1996 to 2021 over Europe. From left to right, trend in TX90p based on air temperatures, trend in TX90p based on soil temperatures, the difference between absolute values of trends in soil and air, and the difference between trends in soil and air where both trends are positive. Results are obtained from mereological stations (a), a combination of the CMSAF remote sensing data and the E-OBS gridded dataset (b) and the ERA5Land reanalysis product (c). Gaps in b) correspond with pixels where the gridded product do not match the criteria for estimating trends (see Methods). Dots indicate areas with significant trends above the 90% confidence level.

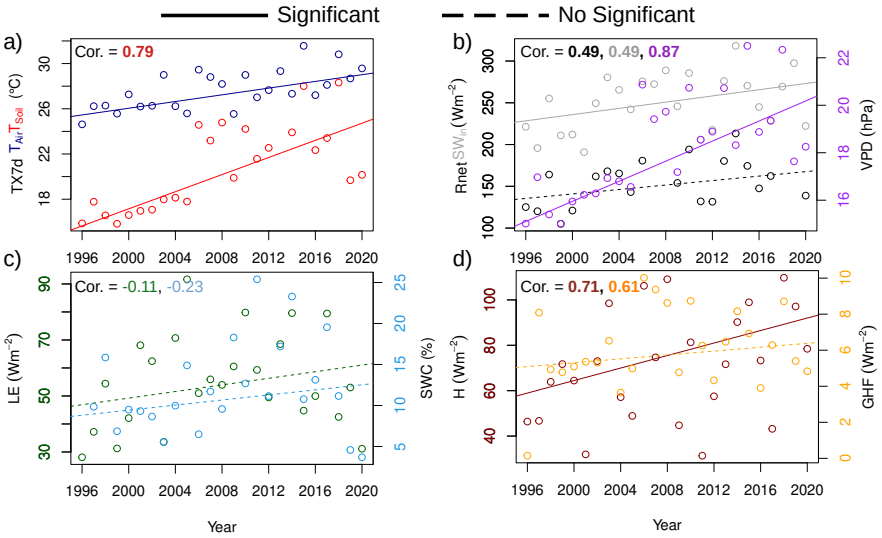

Extended Data Figure 3 | Trends at DE-Tha station during the hottest week per year from 1996 to 2020. a) Trends in TX7d index based on air and soil (2 cm) temperatures during the hottest week per year. b) Mean net radiation (R_{net}), incoming shortwave radiation (SW_{in}) and vapour pressure deficit (VPD) during the hottest week per year. c) Mean latent heat flux (LE) and soil water content in the first 2 cm of the soil (SWC) during the hottest week per year. d) Sensible (H) and ground (GHF) heat flux during the hottest week per year. The hottest week per year for all variables was identified using the TX7d index based on air temperatures. Significant trends above the 90% confidence level are represented with solid lines. Note that although the trend in R_{net} is not significant above the 90% confidence level, it is significant above the 85% confidence level. Numbers in colors indicate the Pearson correlation coefficient of each variable with the TX7d index based on air temperatures, with bold numbers indicating significant correlation above the 90

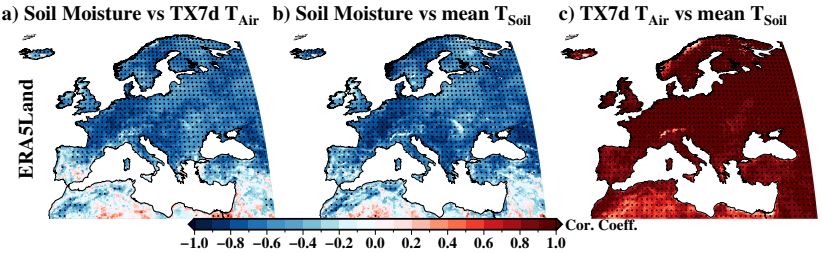

Extended Data Figure 4 | Correlation between soil moisture and temperatures during hot spells. a) Pearson's correlation coefficients between mean soil moisture and the TX7d index based on air temperatures. b) Pearson's correlation coefficients between mean soil moisture and mean soil temperature. c) Pearson's correlation coefficients between mean soil temperature and the TX7d index based on air temperatures. All correlation coefficients were estimated based on the ERA5Land data, using the mean of each variable during the hottest week per year identified by the air TX7d index from 1996 to 2020. Dots correspond with significant areas above the 90% confidence level.

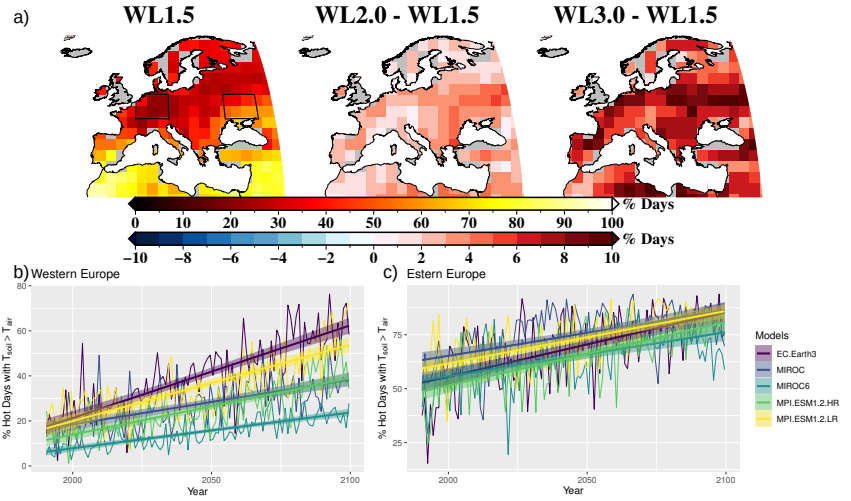

Extended Data Figure 5 | Percentage of days with a release of heat from soil into the atmosphere in summer. a) Percentage of days with daily mean soil temperatures higher than daily mean air temperatures during air hot extremes as represented by the multimodel mean of the CMIP6 models under the 1.5 $°C$ warming level and its difference with warming levels of 2.0 $°C$ and 3.0 $°C$. The average of the percentage of days per year with soil temperatures higher than air temperatures during air hot extremes over central western (b) and eastern (c) Europe (see black rectangles at top left) from 1990 to 2100 for each model separately. Air hot extremes were defined based on the TX90p index.